Chinese Chemical Letters 36 (2025) 110019

Contents lists available at ScienceDirect

Chinese Chemical Letters

journal homepage: www.elsevier.com/locate/cclet

Insight into the effects of C_3H_6 on fresh and hydrothermally aged Cu-SSZ-39 catalysts

Jinpeng Du[a], Junlin Chen[b,c], Yulong Shan[a,**], Tongliang Zhang[a], Yu Sun[a], Zhongqi Liu[a,b], Xiaoyan Shi[a], Wenpo Shan[d], Yunbo Yu[a,b,c,d,*], Hong He[a,b,c,d]

[a] State Key Joint Laboratory of Environment Simulation and Pollution Control, Research Center for Eco-Environmental Sciences, Chinese Academy of Sciences, Beijing 100085, China
[b] University of Chinese Academy of Sciences, Beijing 100049, China
[c] Ganjiang Innovation Academy, Chinese Academy of Sciences, Ganzhou 341119, China
[d] Center for Excellence in Regional Atmospheric Environment, Institute of Urban Environment, Chinese Academy of Sciences, Xiamen 361021, China

ARTICLE INFO

Article history:
Received 29 December 2023
Revised 9 April 2024
Accepted 15 May 2024
Available online 16 May 2024

Keywords:
Diesel vehicle emission
NO_x abatement
NH_3-SCR
Cu-SSZ-39 zeolite
C_3H_6 poisoning

ABSTRACT

Hydrocarbons (HCs), as major poisoning substances, have a crucial influence on NH_3-SCR catalysts. In this work, the effects of C_3H_6 on fresh and hydrothermally aged Cu-SSZ-39 catalysts with different copper contents were investigated. All catalysts suffered a deactivation above 250 °C, especially between 300-400 °C, which was mainly related to the reaction between NH_3 and C_3H_6. However, the hydrothermally aged and the high-copper-loaded Cu-SSZ-39 catalysts could achieve a recovery of NH_3-SCR performance at high temperatures. Such activity recovery was attributed to the oxidation of C_3H_6 by Cu_xO_y species, which therefore inhibited the reaction between NH_3 and C_3H_6. As a result, more NH_3 could be available for the NH_3-SCR reaction and the Cu-SSZ-39 catalysts could maintain a good catalytic activity. Based on these findings, we proposed that high loaded Cu-SSZ-39 catalysts with a little CuO_x formed are preferred for application.

Nitrogen oxides (NO_x) are main air pollutants, and they are detrimental to both environment and human health [1,2]. Abundant amounts of NO_x emitted from diesel vehicles are highly dispersive and hard to control [3,4]. Selective catalytic reduction with ammonia (NH_3-SCR) is one of the most commonly used technologies to abate nitrogen oxide (NO_x) emissions from diesel vehicles [5–8]. Among the various NH_3-SCR catalysts, Cu-based small-pore zeolites have shown extraordinary properties, and Cu-SSZ-13 catalysts are commercially applied in the after-treatment systems of diesel vehicles [9–11].

Cu-SSZ-39 catalysts possess comparable NH_3-SCR activity to Cu-SSZ-13 and much better hydrothermal stability, and thus have a bright future for application [12-14]. Considering the complex composition of the exhaust gas, SCR catalysts usually suffer from a variety of poisoning conditions, such as sulfur poisoning, phosphorus poisoning, alkali/alkaline earth metal poisoning and hydrocarbon (HCs) poisoning [15–17]. Our group has carried out a series of studies on the deactivation mechanisms of Cu-SSZ-39 catalysts [18–20]. The formation of H_2SO_4 and $CuSO_4$ species is the main reason causing low-temperature activity loss in Cu-SSZ-39 catalysts [19]. Alkali/alkaline earth metals were found to induce deterioration of the framework and loss of isolated Cu^{2+} ions, and thus led to serious deactivation. The formation of Cu-P species in phosphorus-poisoned Cu-SSZ-39 catalysts was found to cause a decrease in the number of active copper species and resulted in serious low-temperature deactivation, but such inhibition effect could be alleviated after hydrothermal aging treatment [20]. Understanding the poisoning mechanism provides a guide to improving the resistance of catalysts. However, there is still a lack of understanding of the HCs poisoning mechanism over Cu-SSZ-39 catalysts.

The effects of HCs poisoning on Cu-SSZ-13 catalysts have been widely studied, and C_3H_6 was often chosen as a typical HC compound. Duan *et al.* revealed that C_3H_6 was competitively adsorbed at the active copper sites, and the redox cycle was impeded in the low-temperature range [21]. A similar phenomenon was observed by Ma *et al.* in which active copper sites are covered by C_3H_6 moreover, zeolite pores are blocked by carbon deposits. However, the carbon deposits could be burned off at high temperature and catalytic activity was recovered [22]. Zhao *et al.* further revealed

* Corresponding author at: State Key Joint Laboratory of Environment Simulation and Pollution Control, Research Center for Eco-Environmental Sciences, Chinese Academy of Sciences, Beijing 100085, China.
** Corresponding author.
E-mail addresses: ylshan@rcees.ac.cn (Y. Shan), ybyu@rcees.ac.cn (Y. Yu).

https://doi.org/10.1016/j.cclet.2024.110019
1001-8417/

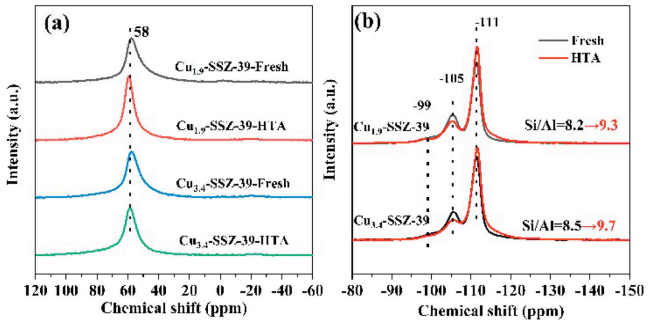

Fig. 1. (a) ^{27}Al and (b) ^{29}Si NMR spectra of Cu-SSZ-39 catalysts with different copper contents before and after hydrothermal aging treatment. Si/Al ratio was calculated from areas of deconvoluted ^{29}Si NMR peaks.

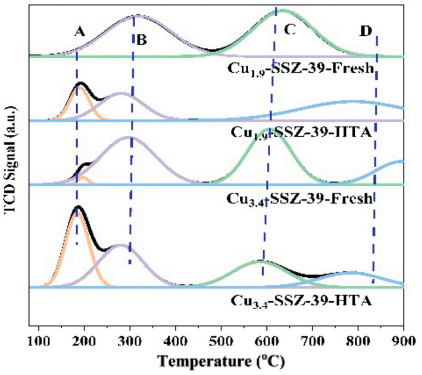

Fig. 2. H_2-TPR profiles of Cu-SSZ-39 catalysts with different copper contents before and after hydrothermal aging treatment.

that the carbon deposits are mainly composed of aliphatic and aromatic compounds, which deepened our understanding of the HCs poisoning mechanism [23]. In our recent study, we thoroughly investigated the C_3H_6 poisoning mechanism of the NH_3-SCR reaction over Cu-SSZ-13 with various Cu contents and Si/Al ratios. It was found that besides the accumulation of carbon deposits, C_3H_6 ammoxidation occurred, which caused a lack of NH_3 and also resulted in a decrease in the high-temperature catalytic activity [24].

In this study, we investigated the effects of C_3H_6 on the catalytic activity of fresh and hydrothermally aged Cu-SSZ-39 catalysts, simulating the short-distance and long-distance driving SCR catalysts. Meanwhile, the influence of Cu content on the C_3H_6 resistance of Cu-SSZ-39 catalysts was discussed, to better understand the C_3H_6 resistance of different Cu species.

The crystallinity of the catalyst was investigated by XRD, and the results are presented in Fig. S1 (Supporting information). $Cu_{1.9}$-SSZ-39-Fresh and $Cu_{3.4}$-SSZ-39-Fresh catalysts both showed the typical diffraction peaks of the AEI structure. After hydrothermal aging treatment, little change in crystallinity was observed, and no characteristic peaks of CuO_x clusters were detected. This indicates that the framework of the prepared catalysts is stable and copper species are highly dispersed in both fresh and aged Cu-SSZ-39 catalysts.

The ^{27}Al NMR and ^{29}Si NMR results of the Cu-SSZ-39 catalysts are shown in Fig. 1. Only a framework Al (FAl) peak at 58 ppm was observed in Fig. 1a, and no extra-framework Al (EFAl) peak at 0 ppm was detected in both fresh and aged Cu-SSZ-39 catalysts [25,26]. Moreover, three peaks at around −111, −105 and −99 ppm were observed in the ^{29}Si NMR profiles (Fig. 1b), and they were assigned to Si(0Al4Si), Si(1Al3Si), and Si(2Al2Si), respectively [25,27]. According to Fig. 1b and Table S1 (Supporting information), a slight increase in Si/Al ratios can be observed in both $Cu_{1.9}$-SSZ-39-Fresh and $Cu_{3.4}$-SSZ-39-Fresh after hydrothermal aging treatment, indicating that weak dealumination occurred [28,29]. Combined with the results of XRD, it can be seen that the framework of the prepared Cu-SSZ-39 catalysts presented good stability.

Copper species, as the active centers in Cu-SSZ-39 catalysts, play an important role in the NH_3-SCR reaction. Therefore, to better understand the effect of C_3H_6 on different Cu species in Cu-SSZ-39 catalysts, H_2-TPR experiments were conducted on both fresh and aged samples, and the results are shown in Fig. 2. The peak B at about 280 °C was attributed to the reduction of Cu^{2+} to Cu^+ in the D6R, and the peaks at temperatures above 500 °C (peak C and peak D) corresponded to the reduction of Cu^+ [30,31]. Only Cu^{2+} and Cu^+ species existed in the $Cu_{1.9}$-SSZ-39-Fresh sample. However, a small peak emerged at around 180 °C (peak A) in $Cu_{3.4}$-SSZ-39-Fresh, assigned to CuO_x species [32]. Moreover, more CuO_x species were formed in $Cu_{1.9}$-SSZ-39-HTA and $Cu_{3.4}$-SSZ-39-HTA.

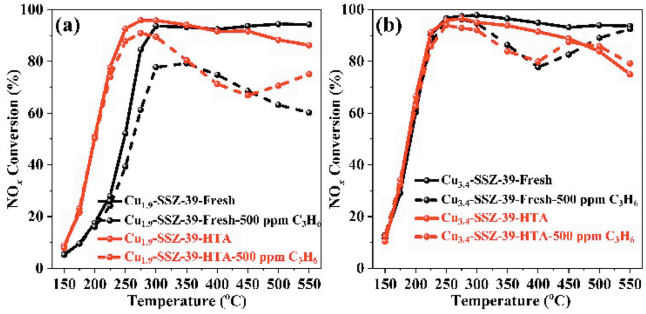

Fig. 3. Effect of C_3H_6 on the activity of Cu-SSZ-39 catalysts with low-copper-loading (a) and high-copper-loading (b) before and after hydrothermal aging. Gas conditions: [NO] = 500 ppm, [NH_3] = 500 ± 5 ppm, [O_2] = [H_2O] = 5 vol%, [C_3H_6] = 500 ppm (when used), balanced by N_2, total gas flow: 500 mL/min, GHSV = 200,000 h^{-1}.

To evaluate the amount of divalent Cu ions in the catalysts, EPR experiments were carried out, with the results depicted in Fig. S2 (Supporting information). Only one type of hexacoordinated Cu^{2+} species ($g_{\|} = 2.41$, $A_{\|} = 133$ G) was observed in both the fresh and aged catalysts, assigned to Cu^{2+} species [13,33]. Moreover, the normalized Cu^{2+} concentration was calculated and the data are presented in Fig. S2b. As can be observed, both $Cu_{1.9}$-SSZ-39-Fresh and $Cu_{3.4}$-SSZ-39-Fresh faced a decrease in the number of Cu^{2+} ions after hydrothermal aging treatment, which indicated that a large amount of Cu^{2+} transformed to EPR-inactive copper species (such as CuO_x).

To sum up, Cu^{2+} species dominated in both the $Cu_{1.9}$-SSZ-39-Fresh and $Cu_{3.4}$-SSZ-39-Fresh catalysts. After hydrothermal aging treatment, part of the Cu^{2+} species transformed to CuO_x species, reducing the concentration of EPR-active Cu^{2+} species.

The influence of C_3H_6 on the fresh and aged Cu-SSZ-39 catalysts with different Cu contents was evaluated, and the results are presented in Fig. 3. After hydrothermal aging treatment, the low-temperature catalytic activity of $Cu_{1.9}$-SSZ-39-HTA significantly increased, while the high-temperature activity slightly decreased. However, the $Cu_{3.4}$-SSZ-39-HTA sample did not achieve an observable increase in low-temperature catalytic activity, while the high-temperature catalytic activity declined, which is in accordance with our previous studies [13,20,32]. After the introduction of C_3H_6, the catalytic activity above 250 °C of $Cu_{1.9}$-SSZ-39-Fresh decreased significantly, with NO_x conversion around 60% at 550 °C. However, the negative affect of C_3H_6 on catalytic activity was alleviated in $Cu_{1.9}$-SSZ-39-HTA, and an increase in NO_x conversion was observed above 450 °C. Meanwhile, the inhibition of catalytic activity in $Cu_{3.4}$-SSZ-39-Fresh caused by C_3H_6 was weaker than that of $Cu_{1.9}$-SSZ-39-Fresh, and the NO_x conversion of $Cu_{3.4}$-SSZ-

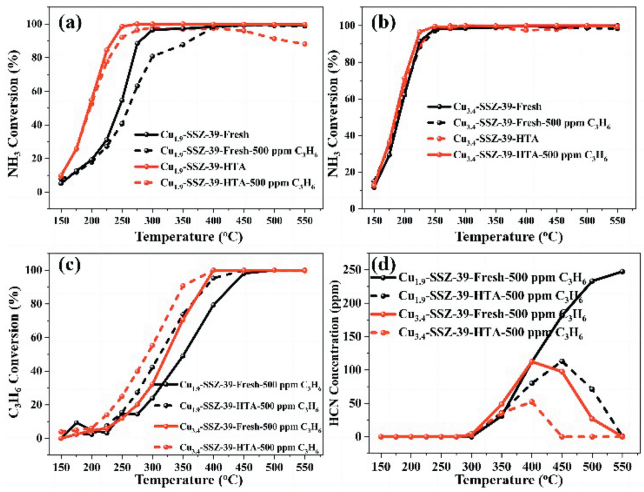

Fig. 4. The NH_3 conversion of Cu-SSZ-39 catalysts with low copper (a) and high copper (b) before and after hydrothermal aging, C_3H_6 conversion (c) and HCN concentration (d). Gas conditions: [NO] = 500 ppm, [NH_3] = 500 ± 5 ppm, [O_2] = [H_2O] = 5 vol%, [C_3H_6] = 500 ppm (when used), balanced by N_2, total gas flow: 500 mL/min, GHSV = 200,000 h^{-1}.

39-Fresh also began to increase above 400 °C. Moreover, the effect of C_3H_6 on catalytic activity was even weaker in $Cu_{3.4}$-SSZ-39-HTA. The NO_x conversion of $Cu_{3.4}$-SSZ-39-HTA-500 ppm C_3H_6 was even higher than that of $Cu_{3.4}$-SSZ-39-HTA above 450 °C.

To better understand the poisoning mechanism of C_3H_6 on Cu-SSZ-39 catalysts, NH_3 conversion, C_3H_6 conversion and the concentration of HCN during NH_3-SCR activity tests are depicted in Fig. 4. The shapes of the NH_3 conversion curves of $Cu_{1.9}$-SSZ-39-Fresh and $Cu_{1.9}$-SSZ-39-HTA are similar to their NO_x conversion curves, while the NH_3 conversion of $Cu_{1.9}$-SSZ-39-HTA was slightly higher than NO_x conversion over 450 °C (Figs. 4a and b). Considering the formation of CuO_x species in $Cu_{1.9}$-SSZ-39-HTA (Fig. 2), the decline in NO_x conversion at high temperature was probably due to non-selective oxidation of NH_3. In the presence of C_3H_6, the NH_3 conversion of $Cu_{1.9}$-SSZ-39-Fresh and $Cu_{1.9}$-SSZ-39-HTA was clearly higher than NO_x conversion, especially over 350 °C. This result indicates that NH_3 was consumed by other reactions, and not enough NH_3 participated in the reduction of NO_x. Meanwhile, the C_3H_6 conversion of $Cu_{1.9}$-SSZ-39-Fresh and $Cu_{1.9}$-SSZ-39-HTA during NH_3-SCR tests is presented in Fig. 4c. The ignition temperature of C_3H_6 in $Cu_{1.9}$-SSZ-39-Fresh and $Cu_{1.9}$-SSZ-39-HTA is around 300–350 °C, and as the conversion of C_3H_6 increased, HCN began to form, as presented in Fig. 4d. Therefore, it can be inferred that the NH_3 reacted with C_3H_6 over 300 °C, forming HCN according to Eq. 1 [17,34], and the amount of NH_3 was insufficient for the NH_3-SCR reaction. It is worth mentioning that $Cu_{1.9}$-SSZ-39-HTA possessed higher C_3H_6 conversion than $Cu_{1.9}$-SSZ-39-Fresh, while more HCN formed for $Cu_{1.9}$-SSZ-39-Fresh, indicating that part of the C_3H_6 was consumed by other reactions for $Cu_{1.9}$-SSZ-39-HTA. Furthermore, the concentration of HCN over $Cu_{1.9}$-SSZ-39-HTA began to decrease over 450 °C (Fig. 4d), accompanied by an increase in NO_x conversion (Fig. 3a). This indicates that the reaction between C_3H_6 and NH_3 was hindered in $Cu_{1.9}$-SSZ-39-HTA over 450 °C, so that sufficient NH_3 was available to participate in the NH_3-SCR reaction.

$$C_3H_6 + 3NH_3 + 3O_2 \rightarrow 3HCN + 6H_2O \quad (1)$$

The NH_3 conversion of $Cu_{3.4}$-SSZ-39-Fresh and $Cu_{3.4}$-SSZ-39-HTA is illustrated in Fig. 4b. The NH_3 conversion of $Cu_{3.4}$-SSZ-39-Fresh was similar to its NO_x conversion, however, $Cu_{3.4}$-SSZ-39-HTA possessed higher NH_3 conversion than NO_x conversion over 350 °C, owing to the existence of CuO_x species. When C_3H_6 was introduced, the NH_3 conversion of both $Cu_{3.4}$-SSZ-39-Fresh and $Cu_{3.4}$-SSZ-39-HTA was higher than NO_x conversion over 300 °C. From 300 °C to 400 °C, C_3H_6 conversion rose dramatically meanwhile, the HCN concentration increased and NO_x conversion decreased. In this temperature range NH_3 reacted with C_3H_6 therefore, the NH_3-SCR reaction was hindered. When the temperature rose over 450 °C, the HCN concentration decreased and NO_x conversion recovered, indicating that C_3H_6 was consumed by other reactions and more NH_3 participated in the NH_3-SCR reaction.

It should be noted that HC-SCR is also a way for NO_x removal [35,36], and the reaction between C_3H_6 and NO followed Eq. 2. Therefore, the C_3H_6-SCR reaction was conducted to evaluate its impact on the NH_3-SCR reaction over Cu-SSZ-39 catalysts. Fig. S3a (Supporting information) shows that the NO_x conversion was quite low below 300 °C during the C_3H_6-SCR reaction in all the tested Cu-SSZ-39 catalysts. Meanwhile, NO_x conversion began to increase over 300 °C, together with the formation of a small amount of HCN (Fig. S3b in Supporting information). The formation of HCN may have followed Eq. 3, and the concentration of HCN (Fig. S3b) was lower than that generated in the NH_3-SCR reaction (Fig. 4d). Considering that the inlet concentration of NO was 500 ppm, less than 8% NO_x conversion was obtained for $Cu_{1.9}$-SSZ-39-Fresh, and the HCN concentration was over 20 ppm at 400 and 450 °C. Therefore, over half of the NO_x was consumed following Eq. 3 for $Cu_{1.9}$-SSZ-39-Fresh at 400 and 450 °C. However, for the other catalysts, most of the NO_x was consumed following Eq. 2, and C_3H_6-SCR played an important role in the NO_x conversion over 350 °C.

$$2C_3H_6 + 4NO + 7O_2 \rightarrow 2N_2 + 6CO_2 + 6H_2O \quad (2)$$

$$4C_3H_6 + 4NO + 11O_2 \rightarrow 4HCN + 8CO_2 + 10H_2O \quad (3)$$

To further prove the side reaction between NH_3 and C_3H_6 led to a deficiency in the amount of NH_3 available for the NH_3-SCR reaction, NH_3 was introduced at various concentrations during the NH_3-SCR tests. As presented in Figs. 5a and b, both fresh $Cu_{1.9}$-SSZ-39 and $Cu_{3.4}$-SSZ-39 catalysts faced a decline in NO_x conversion when C_3H_6 was introduced regardless of the NH_3 concentration. When the NH_3 concentration increased from 400 ppm to 500 ppm, the NO_x conversion for both the $Cu_{1.9}$-SSZ-39-Fresh and $Cu_{3.4}$-SSZ-39-Fresh catalysts increased dramatically. However, the NO_x conversion was only slightly improved when the NH_3 concentration further increased to 600 ppm. Similar phenomenon was observed in the aged catalysts as presented in Figs. 5c and d. When C_3H_6 was introduced, NO_x conversion declined in both $Cu_{1.9}$-SSZ-39-HTA and $Cu_{3.4}$-SSZ-39-HTA catalysts; with the increase of NH_3 concentration from 400 ppm to 500 ppm NO_x conversion was improved significantly.

HCN concentration of catalysts was helpful to analyze side reactions and the results were presented in Figs. 5e and f. More HCN was generated when the NH_3 concentration increased, which indicated that the additional NH_3 was depleted by C_3H_6. For the $Cu_{3.4}$-SSZ-39 catalyst, NO_x conversion decreased from 300 °C to 400 °C, and further increased from 450 °C on. This was in accordance with the turning point of HCN concentration at 400 °C as presented in Fig. 5f. This phenomenon indicates that when HCN formed (from C_3H_6 reacting with NH_3), the NH_3-SCR reaction was hindered; when the HCN concentration decreased (C_3H_6 was consumed by other reactions), the NH_3-SCR reaction recovered. The relationship between HCN generation and NO_x conversion indicates that C_3H_6 hindered the NH_3-SCR reaction by depleting NH_3. $Cu_{1.9}$-SSZ-39-HTA exhibited similar NO_x conversion and HCN concentration curves to those of $Cu_{3.4}$-SSZ-39-Fresh, which was probably due to the composition of Cu species in them being similar

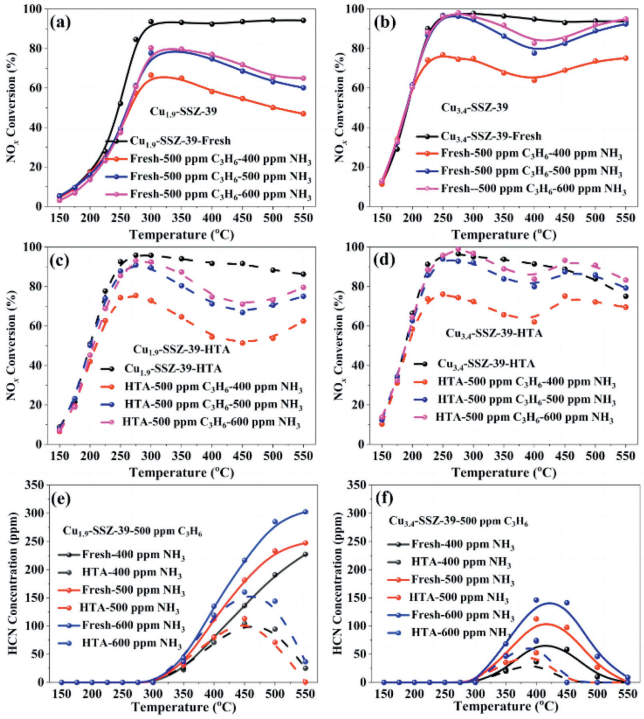

Fig. 5. NO_x conversion of Cu-SSZ-39 catalysts using different NH_3 concentrations: (a) $Cu_{1.9}$-SSZ-39-Fresh, (b) $Cu_{3.4}$-SSZ-39-Fresh, (c) $Cu_{1.9}$-SSZ-39-HTA, (d) $Cu_{3.4}$-SSZ-39-HTA. HCN concentration: (e) $Cu_{1.9}$-SSZ-39, (f) $Cu_{3.4}$-SSZ-39 catalysts. Gas conditions: $[NH_3] = 400$, 500, 600 ppm, $[NO] = 500$ ppm, $[O_2] = [H_2O] = 5$ vol%, $[C_3H_6] = 500$ ppm, balanced by N_2, total gas flow: 500 mL/min, GHSV = 200,000 h^{-1}.

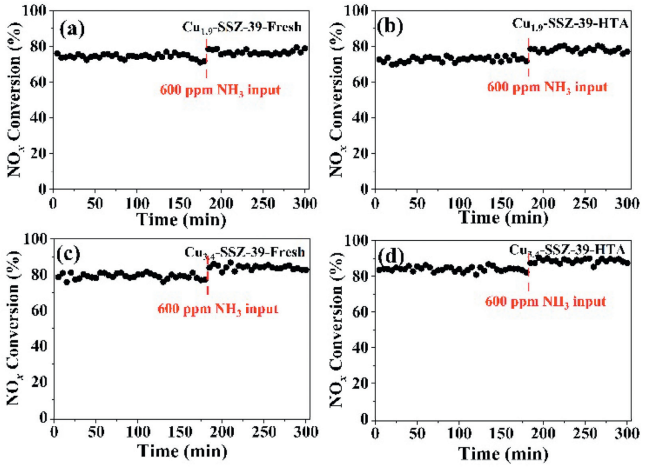

Fig. 6. NO_x conversion of Cu-SSZ-39 at 400 °C. (a) $Cu_{1.9}$-SSZ-39-Fresh, (b) $Cu_{1.9}$-SSZ-39-HTA, (c) $Cu_{3.4}$-SSZ-39-Fresh and (d) $Cu_{3.4}$-SSZ-39-HTA. Gas conditions: $[NH_3] = 500$ ppm, $[C_3H_6] = 500$ ppm, 600 ppm, $[O_2] = [H_2O] = 5$ vol%, balanced by N_2, total gas flow: 500 mL/min, GHSV = 200,000 h^{-1}.

(both had a small amount of CuO_x species). However, $Cu_{3.4}$-SSZ-39-HTA possessed much more CuO_x species, and the NO_x conversion curve was somewhat different. Besides the turning point at 400 °C, another turning point at 450 °C emerged in the NO_x conversion curve of $Cu_{3.4}$-SSZ-39-HTA. As presented in Figs. 5e and f, the least amount of HCN was generated compared with the other tested catalysts. Therefore, the decrease in NO_x conversion over 450° in $Cu_{3.4}$-SSZ-39-HTA was probably due to the non-selective oxidation of NH_3.

In addition, to investigate whether carbon deposition contributed to the decline in NO_x conversion activity at high temperatures, steady-state NH_3-SCR testing was carried out. Both fresh and aged Cu-SSZ-39 catalysts with different Cu content were exposed to a NH_3-SCR+C_3H_6 atmosphere at 400 °C, and the resulting NO_x conversion is presented in Fig. 6. In the first 180 min, the NO_x conversion of all the tested catalysts remained constant without a detectable decline trend, excluding the effect of carbon deposition under the conditions we used. The concentration of input NH_3 was increased from 500 ppm to 600 ppm at the 180th min, and an increase in NO_x conversion could be observed for all tested catalysts. This was in accordance with the result of Fig. 5, which further proved that the depletion of NH_3 was the main reaction for the decline in NO_x conversion.

In order to further investigate the side reaction, NH_3 (+C_3H_6) oxidation experiments were conducted, and results are shown in Fig. S4 (Supporting information). The NH_3 conversion of the fresh and aged $Cu_{1.9}$-SSZ-39 catalysts was below 50% under the entire tested temperature range without C_3H_6 introduction (Fig. S4a). When C_3H_6 was introduced, the NH_3 conversion of $Cu_{1.9}$-SSZ-39 catalysts began to increase significantly over 400 °C, and a large amount of HCN species formed for $Cu_{1.9}$-SSZ-39-Fresh (Figs. S4a and b). The NH_3 conversion of $Cu_{3.4}$-SSZ-39 was not over 50% above 500 °C without C_3H_6. When C_3H_6 was introduced, more NH_3 was consumed at 400 and 450 °C and large amount of HCN was produced (Figs. S4b and c). However, $Cu_{3.4}$-SSZ-39-HTA exhibited higher NH_3 conversion without C_3H_6, and hardly any HCN formed with $Cu_{3.4}$-SSZ-39-HTA when C_3H_6 was introduced (Figs. S4b and c). This indicates that NH_3 was not consumed by C_3H_6, and non-selective oxidation of NH_3 was the main reason for the high NH_3 conversion of $Cu_{3.4}$-SSZ-39-HTA. Meanwhile, $Cu_{3.4}$-SSZ-39-HTA exhibited the highest C_3H_6 conversion among the tested catalysts, indicating that the oxidation of C_3H_6 is also more facile with this catalyst. Moreover, C_3H_6 conversion was presented in Fig. S4d, and C_3H_6 conversion of prepared catalysts followed sequence as: $Cu_{3.4}$-SSZ-39-HTA > $Cu_{3.4}$-SSZ-39-Fresh > $Cu_{1.9}$-SSZ-39-HTA > $Cu_{1.9}$-SSZ-39-Fresh. Considering the Cu species in prepared catalysts, it can be deduced that CuO_x species promoted C_3H_6 oxidation.

As presented in Fig. 3, little effect of C_3H_6 was observed on the catalytic activity of Cu-SSZ-39 catalysts below 250 °C, and the negative affect on catalytic performance mainly occurred at high temperatures. The diffusion diameter of C_3H_6 molecules is around 4.5 Å, but the pore size of Cu-SSZ-39 zeolites is 3.84 Å × 3.84 Å × 3.64 Å. Therefore, it is difficult for C_3H_6 molecules to enter the pore channels of Cu-SSZ-39 catalysts and effect catalytic activity below 250 °C [37,38]. With increasing temperature, the thermal vibrations of the zeolite framework and C_3H_6 molecules were intensified simultaneously [39,40]. Therefore, C_3H_6 molecules could enter the channels of the Cu-SSZ-39 zeolite and affect the catalytic activity of the Cu-SSZ-39 catalysts.

The effects of C_3H_6 on the catalytic activity of Cu-SSZ-39 catalysts with different Cu loadings varied significantly. As presented in Fig. 3, NO_x conversion was inhibited by C_3H_6 for both $Cu_{1.9}$-SSZ-39-Fresh and $Cu_{3.4}$-SSZ-39-Fresh above 250 °C. However, the activity loss was much more severe for $Cu_{1.9}$-SSZ-39-Fresh, and an increase in NO_x conversion was even observed for $Cu_{3.4}$-SSZ-39-Fresh over 400 °C. H_2-TPR results (Fig. 2) revealed that CuO_x species emerged in $Cu_{3.4}$-SSZ-39-Fresh, which may explain the difference between $Cu_{1.9}$-SSZ-39-Fresh and $Cu_{3.4}$-SSZ-39-Fresh. As presented in Figs. 4c and d, C_3H_6 conversion was higher in $Cu_{3.4}$-SSZ-39-Fresh with less HCN formation, indicating that oxidation of C_3H_6 occurred more easily when Cu loading was high. Moreover, we have concluded that the reaction between C_3H_6 and NH_3 was the main reason for catalytic activity loss at high temperature. $Cu_{3.4}$-SSZ-39-Fresh, with more CuO_x, can more easily oxidize C_3H_6 therefore, more NH_3 can participate in the NH_3-SCR reaction, and it possessed better catalytic performance than $Cu_{1.9}$-SSZ-39-Fresh.

Hydrothermal aging treatment also affected the C_3H_6 resistance of Cu-SSZ-39 catalysts. As presented in Fig. 3, C_3H_6 had less effect on the catalytic activity of the aged Cu-SSZ-39 catalysts than the fresh ones. Meanwhile, higher C_3H_6 conversion and lower HCN production was achieved by the aged Cu-SSZ-39 catalysts (Figs. 4c and d). Similar to $Cu_{3.4}$-SSZ-39-Fresh, both $Cu_{1.9}$-SSZ-39-HTA and $Cu_{3.4}$-SSZ-39-HTA possess CuO_x species, as shown in Fig. 2. Meanwhile, a turning point of NO_x conversion emerged for $Cu_{3.4}$-SSZ-39-Fresh, $Cu_{1.9}$-SSZ-39-HTA and $Cu_{3.4}$-SSZ-39-HTA around 400 °C (Fig. 3). As we discussed above, CuO_x species are active for C_3H_6 oxidation over 400 °C, which alleviates the reaction between C_3H_6 and NH_3 [41]. Therefore, NH_3 is released to participate in the NH_3-SCR reaction, resulting in an increase in NO_x conversion. When Cu-SSZ-39 catalysts are hydrothermally aged, abundant CuO_x species form therefore, catalytic activity recovers. It is worth mentioning that a further decrease in NO_x conversion was observed in $Cu_{3.4}$-SSZ-39-HTA above 500 °C (Fig. 3b). This is because the presence of excessive CuO_x species could also increase the oxidation of NH_3 (Fig. S4b), which again resulted in a lack of NH_3 [42,43].

It is interesting that Cu-SSZ-13 catalysts behaved differently when subjected to C_3H_6 poisoning. Studies revealed a decrease in low-temperature catalytic activity when C_3H_6 was introduced to Cu-SSZ-13, and the blocking of pores by carbon deposits was the main reason for activity loss [21-23,44]. In our recent study, we found that besides the propylene ammoxidation reaction, carbon deposits were also responsible for the activity loss of Cu-SSZ-13. Meanwhile, carbon can be deposited from 250 °C to 500 °C [24]. However, the decline in NO_x conversion for Cu-SSZ-39 was not due to carbon deposits in this study. As presented in Fig. 6, no decline in NO_x conversion was observed with the introduction of C_3H_6 for any of the Cu-SSZ-39 catalysts within 180 min. Comparatively, small-pore zeolites possess better HC resistance than medium- or large-pore zeolites, because HC molecules are too large to enter the zeolite pores. Moreover, compared with Cu-SSZ-13, the channels of Cu-SSZ-39 are more tortuous, therefore C_3H_6 molecules have more difficulty entering the channels of Cu-SSZ-39 under the conditions we carried out, avoiding carbon deposition. Furthermore, the CuO_x species in Cu-SSZ-39 catalysts possessed better redox ability than Cu^{2+} species [32]. Therefore, CuO_x species in Cu-SSZ-39 can help to oxidize C_3H_6, preserving NH_3 for the NH_3-SCR reaction.

In this study, the effect of C_3H_6 on Cu-SSZ-39 catalysts was investigated. It turned out the propylene ammonia oxidation reaction at high temperatures resulted in the consumption of NH_3, therefore, affecting NH_3-SCR activity. CuO_x species in high Cu loaded or hydrothermally aged Cu-SSZ-39 catalysts facilitated the oxidation of C_3H_6, preserving NH_3 for SCR reaction. As a result, catalyst with higher Cu content performed better with C_3H_6 existing, meanwhile, long-distance driving (hydrothermal aging process) cannot result in the decline of HC resistance in Cu-SSZ-39 catalysts. For one thing, Cu-SSZ-39 catalysts are known for excellent hydrothermal stability, and the aged catalysts even presented better HCs resistance, which proved that Cu-SSZ-39 is capable of application. For another, according to the results of this study, Cu-SSZ-39 catalysts of high Cu content with a little CuO_x species should be used considering SCR activity and HCs resistance. The research on the HCs resistance of Cu-SSZ-39 catalysts proved that Cu-SSZ-39 catalysts are capable of application in diesel vehicles. The application of Cu-SSZ-39 catalysts can help to further improving atmospheric environment.

Declaration of competing interest

The authors declare that they have no known competing financial interests or personal relationships that could have appeared to influence the work reported in this paper.

CRediT authorship contribution statement

Jinpeng Du: Data curation, Formal analysis, Investigation, Methodology, Writing – original draft, Writing – review & editing, Funding acquisition. **Junlin Chen:** Data curation, Formal analysis, Investigation, Methodology, Writing – original draft. **Yulong Shan:** Conceptualization, Data curation, Resources, Supervision, Writing – review & editing, Funding acquisition. **Tongliang Zhang:** Investigation, Validation. **Yu Sun:** Data curation, Investigation, Validation. **Zhongqi Liu:** Data curation, Formal analysis, Validation. **Xiaoyan Shi:** Data curation, Formal analysis. **Wenpo Shan:** Data curation, Validation. **Yunbo Yu:** Data curation, Funding acquisition, Resources, Supervision, Validation, Writing – review & editing. **Hong He:** Project administration, Resources, Validation.

Acknowledgments

This work was financially supported by the National Natural Science Foundation of China (Nos. 52200136, 52270112). National Energy-Saving and Low-Carbon Materials Production and Application Demonstration Platform Program (No. TC220H06N). Young Elite Scientists Sponsorship Program by CAST (No. 2022QNRC001).

Supplementary materials

Supplementary material associated with this article can be found, in the online version, at doi:10.1016/j.cclet.2024.110019.

References

[1] T. Chen, P. Zhang, Q. Ma, et al., Environ. Sci. Technol. 56 (2022) 13654–13663.
[2] Y. Jiang, D. Ding, Z. Dong, et al., Environ. Sci. Technol. 57 (2023) 4424–4433.
[3] G.A. Bishop, M.J. Haugen, B.C. McDonald, A.M. Boies, Environ. Sci. Technol. 56 (2022) 1885–1893.
[4] H. Kong, J. Lin, L. Chen, et al., Environ. Sci. Technol. 56 (2022) 7131–7142.
[5] W. Shan, H. Song, Catal. Sci. Technol. 5 (2015) 4280–4288.
[6] Q. Yan, R. Yang, Y. Zhang, et al., Environ. Prog. Sustain. 35 (2016) 1061–1069.
[7] Y. Shan, J. Du, Y. Zhang, et al., Natl. Sci. Rev. 8 (2021) nwab010.
[8] Q. Wang, M. Shen, J. Wang, C. Wang, J. Wang, J. Rare Earths. 39 (2021) 548–557.
[9] J.H. Kwak, R.G. Tonkyn, D.H. Kim, et al., J. Catal. 275 (2010) 187–190.
[10] M. Iwamoto, H. Furukawa, S. Kagawa, Stud. Surf. Sci. Catal. 28 (1986) 943–949.
[11] D. Deng, S. Deng, D. He, et al., J. Rare Earths 39 (2021) 969–978.
[12] M. Moliner, C. Franch, E. Palomares, M. Grill, A. Corma, Chem. Commun. 48 (2012) 8264–8266.
[13] Y. Shan, W. Shan, X. Shi, et al., Appl. Catal. B: Environ. 264 (2020) 118511–118520.
[14] Y. Wang, J. Li, Z. Liu, Appl. Catal. B: Environ. 343 (2024) 123479–123498.
[15] J.E. Schmidt, R. Oord, W. Guo, J.D. Poplawsky, B.M. Weckhuysen, Nat. Commun. 8 (2017) 1666.
[16] K. Xie, K. Leistner, K. Wijayanti, et al., Catal. Today. 297 (2017) 46–52.
[17] I. Heo, S. Sung, M.B. Park, et al., ACS Catal. 9 (2019) 9800–9812.
[18] N. Zhu, W. Shan, Y. Shan, et al., Chem. Eng. J. 388 (2020) 124250.
[19] J. Du, Y. Shan, G. Xu, et al., Catal. Sci. Technol. 10 (2020) 1256–1263.
[20] J. Chen, Y. Shan, Y. Sun, et al., Environ. Sci. Technol. 57 (2023) 4113–4121.
[21] Y. Duan, L. Wang, Y. Zhang, W. Du, Y. Zhang, Catalysts 11 (2021) 1327.
[22] L. Ma, W. Su, Z. Li, et al., Catal. Today 245 (2015) 16–21.
[23] H. Zhao, X. Wu, Z. Huang, et al., Energ. Fuels 36 (2022) 2712–2721.
[24] W. Ding, Y. Sun, J. Liu, et al., Chem. Eng. J. 483 (2024) 149272.
[25] R. Li, Y. Zhu, Z. Zhang, et al., Appl. Catal. B: Environ. 283 (2021) 119641.
[26] R. Osuga, T. Takeuchi, M. Sawada, et al., Catal. Sci. Technol. 11 (2021) 5839–5848.
[27] Q. Lin, S. Xu, H. Zhao, et al., ACS Catal. 12 (2022) 14026–14039.
[28] F. Dogan, K.D. Hammond, G.A. Tompsett, et al., J. Am. Chem. Soc. 131 (2009) 11062–11079.
[29] J. Klinowski, Chem. Rev. 91 (1991) 1459–1479.
[30] S. Zhang, S. Ming, L. Guo, et al., J. Hazard. Mater. 414 (2021) 125543.
[31] L. Guo, S. Ming, S. Zhang, et al., Ind. Eng. Chem. Res. 59 (2020) 21275–21285.
[32] J. Du, Y. Shan, Y. Sun, et al., Appl. Catal. B: Environ. 294 (2021) 120237.
[33] Y.J. Kim, J.K. Lee, K.M. Min, et al., J. Catal. 311 (2014) 447–457.
[34] J. Liu, X. Shi, Y. Yu, et al., Appl. Catal. B: Environ. 324 (2023) 122283.
[35] J. Xu, Y. Qin, H. Wang, F. Guo, J. Xie, New. J. Chem. 44 (2020) 817–831.
[36] H. He, X. Zhang, Q. Wu, C. Zhang, Y. Yu, Catal. Surv. Asia 12 (2008) 38–55.
[37] L. Ma, J. Li, Y. Cheng, C.K. Lambert, L. Fu, Environ. Sci. Technol. 46 (2012) 1747–1754.

[38] J.E. Schmidt, L. Peng, A.L. Paioni, et al., J. Am. Chem. Soc. 140 (2018) 9154–9158.
[39] X. Cheng, Z. Li, Y.L. He, RSC Adv. 9 (2019) 9546–9554.
[40] P.K. Chaudhary, R. Arundhathi, M.W. Kasture, et al., Roy. Soc. Open. Sci. 10 (2023) 230524.
[41] Y. Lu, L. Duan, Z. Sun, J. Chen, P. Combust. Inst. 38 (2021) 6513–6520.
[42] S. Han, J. Cheng, C. Zheng, et al., Appl. Surf. Sci. 419 (2017) 382–392.
[43] R. Li, X. Jiang, J. Lin, et al., Chem. Eng. J. 441 (2022) 136021.
[44] A. Wang, Y. Wang, E.D. Walter, et al., Catal. Today 320 (2019) 91–99.